Decision–Feedback Subset Multiple–Symbol Differential Detection for Unitary Space–Time Modulation

Volker Pauli, Johannes Huber, *Fellow, IEEE*, and Lutz Lampe, *Senior Member, IEEE*

Abstract— In this letter, a novel noncoherent detection algorithm for differential space–time modulation (DSTM) over flat fading multiple–input multiple–output channels is presented. This algorithm, which is referred to as decision–feedback subset multiple–symbol differential detection (DF–S–MSDD), combines ideas from decision–feedback differential detection (DFDD) and subset multiple–symbol differential detection (S–MSDD). More specifically, the DF–S–MSDD decision metric includes a number of previous decisions (i.e. decision feedback) and the optimization over the remaining hypothetical symbols returns decisions only for a subset of these (i.e. S–MSDD). Furthermore, an implementation of DF–S–MSDD based on tree–search (TS) methods is devised. Due to the concept of subset detection, DF–S–MSDD outperforms MSDD in terms of error–rate performance. At the same time, due to the use of decision feedback, it also requires lower computational complexity than the TS–based MSDD schemes for DSTM proposed recently in the literature.

Index Terms— Differential space–time modulation (DSTM), multiple–symbol differential detection (MSDD), decision–feedback differential detection (DFDD), noncoherent detection, fading channels.

I. INTRODUCTION

Differential space–time modulation (DSTM) using unitary–matrix signal constellations is an attractive solution for transmission over multiple–input multiple–output (MIMO) fading channels with noncoherent detection, which obviates channel estimation at the receiver [1]–[3]. To achieve good error–rate performance with DSTM also in relatively fast MIMO fading channels, appropriate receiver processing techniques have to be applied. These can be roughly categorized into noncoherent sequence detection (NSD) and block–based detection, where for the latter multiple–symbol differential detection (MSDD) and decision–feedback differential detection (DFDD) are the most popular schemes. In NSD the entire transmit sequence is detected based on a limited tree search (e.g. [4]) or reduced–state Viterbi decoding (e.g. [5]–[9]). In MSDD (e.g. [10]–[12]) the transmitted data is estimated in blocks of $N-1$ consecutive symbols based on the observation of N received symbols. To reduce the complexity of MSDD, methods from

tree–search (TS) decoding have been adopted in e.g. [13]–[15]. While these TS–based algorithms greatly reduce the average complexity compared to a brute–force search, they have a number of drawbacks: (i) their average computational complexity may become prohibitively large in *low signal–to–noise ratios (SNRs)* and (ii) their *instantaneous* computational complexity is a random variable depending on the instantaneous channel realization. DFDD (e.g. [16]–[18]), on the other hand, uses decision feedback of $N-2$ previous symbols to detect only the current symbol and thus complexity is relatively low and constant, independent of SNR and channel realization. On the negative side, DFDD leaves a gap in power efficiency (SNR required to achieve a certain error rate) compared to MSDD.

In this letter, we propose a novel algorithm for block–based noncoherent detection, which combines elements from MSDD and DFDD. More specifically, partial decision feedback of between 1 and $N-2$ symbols is employed and MSDD is performed for the remaining symbols. Furthermore, motivated by the observation that estimates of symbols at the edges of the MSDD window are rather unreliable, decisions are made only on a subset of data symbols. We refer to this algorithm as decision–feedback subset multiple–symbol differential detection (DF–S–MSDD) and also devise a TS–based implementation for it. Numerical results show that DF–S–MSDD is capable of achieving lower error rates than MSDD with the same observation window length. Furthermore, its TS–based implementation is advantageous over existing TS–based MSDD algorithms (cf. [13]–[15]) in that (i) its average computational complexity is less dependent on the SNR and (ii) its instantaneous complexity can be limited to values comparable to the average complexity without negative impact on the performance.

Organization: The remainder of this letter is organized as follows. Section II introduces the system model and MSDD decision rule. The new DF–S–MSDD is presented in Section III. Numerical results are shown and discussed in Section IV, and conclusions are given in Section V.

Notation: Throughout this letter we use the following notation. Bold upper case $\boldsymbol{X}$ denote matrices. $(\cdot)^{\mathsf{H}}$, $\mathrm{tr}\{\cdot\}$, $\|\cdot\|$, $\otimes$, and $\mathcal{E}\{\cdot\}$ denote Hermitian transposition, trace, Frobenius norm, Kronecker product, and expectation, respectively. $\boldsymbol{I}_L$ is the $L \times L$ identity matrix and $\mathrm{diag}\{\boldsymbol{X}_1, \ldots, \boldsymbol{X}_L\}$ is an $LM \times LN$ block–diagonal matrix with the $M \times N$ matrices $\boldsymbol{X}_l$ on its main diagonal. A *symmetric* $L \times L$ Toeplitz matrix is defined by $\mathrm{toeplitz}\{x_1, \ldots, x_L\}$.

II. PRELIMINARIES

In this section, we briefly introduce the MIMO system model for DSTM with MSDD, and we state the maximum–likelihood (ML) decision rule for MSDD.

A. System Model

We consider transmission using N_T transmit and N_R receive antennas. At the transmitter $N_\mathrm{T} R$ bits are mapped to $N_\mathrm{T} \times N_\mathrm{T}$ unitary matrices $\boldsymbol{V}[k]$ which are taken from a set $\mathcal{V} \triangleq \{\boldsymbol{V}^{(l)} \,|\, l \in \{1, \dots, L\}, L \triangleq 2^{N_\mathrm{T} R}\}$. R is the data rate in bit per channel use. In order to facilitate noncoherent detection the data symbols $\boldsymbol{V}[k]$ are differentially encoded into transmit symbols

$$\boldsymbol{S}[k] = \boldsymbol{V}[k]\boldsymbol{S}[k-1], \ \boldsymbol{S}[0] = \boldsymbol{I}_{N_\mathrm{T}}. \tag{1}$$

The $N_\mathrm{T} \times N_\mathrm{T}$ matrices $\boldsymbol{S}[k]$ are transmitted in a row–by–row fashion from the N_T transmit antennas in N_T successive modulation intervals (cf. e.g. [1]–[3]).

While the transmission channel changes continuously with time, the design of low–complexity noncoherent detectors is based on the assumption of quasi–static fading, i.e. the channel is assumed to be constant during N_T consecutive modulation intervals.[1] In this case, the received signal $\boldsymbol{R}[k]$ corresponding to the transmission of one DSTM symbol $\boldsymbol{S}[k]$ can be described via

$$\boldsymbol{R}[k] = \boldsymbol{S}[k]\boldsymbol{H}[k] + \boldsymbol{N}[k], \tag{2}$$

where $\boldsymbol{H}[k]$ denotes the $N_\mathrm{T} \times N_\mathrm{R}$ matrix of i.i.d. circularly symmetric complex Gaussian fading gains with temporal auto-correlation function $\psi_{hh}[\kappa] \triangleq \mathcal{E}\{h_{i,j}[k+\kappa]h_{i,j}^*[k]\}$ and $\boldsymbol{N}[k]$ models additive spatially and temporally white Gaussian noise with variance σ_n^2.

B. Maximum–Likelihood Multiple–Symbol Differential Detection (ML–MSDD)

MSDD processes blocks $\bar{\boldsymbol{R}}[k] \triangleq \big[\boldsymbol{R}^\mathsf{H}[k-N+1], \dots, \boldsymbol{R}^\mathsf{H}[k]\big]^\mathsf{H}$ of N consecutively received matrix symbols at a time to determine blocks $\hat{\bar{\boldsymbol{V}}}[k] \triangleq \big[\hat{\boldsymbol{V}}^\mathsf{H}[k-N+2], \dots, \hat{\boldsymbol{V}}^\mathsf{H}[k]\big]^\mathsf{H}$ of $N-1$ data symbols. The ML decision rule is given by (e.g. [15])

$$\hat{\bar{\boldsymbol{V}}}[k] = \operatorname*{argmin}_{\tilde{\bar{\boldsymbol{V}}}[k]\in\mathcal{V}^{N-1}} \left\{ \operatorname{tr}\left\{ \bar{\boldsymbol{R}}^\mathsf{H}[k]\tilde{\bar{\boldsymbol{S}}}_\mathrm{D}[k]\left(\boldsymbol{C}^{-1}\otimes\boldsymbol{I}_{N_\mathrm{T}}\right)\tilde{\bar{\boldsymbol{S}}}_\mathrm{D}^\mathsf{H}[k]\bar{\boldsymbol{R}}[k] \right\} \right\} \tag{3}$$

where

$$\boldsymbol{C} \triangleq \left(\boldsymbol{\Psi}_{\boldsymbol{hh}} + \sigma_n^2\boldsymbol{I}_N\right), \tag{4}$$

$$\boldsymbol{\Psi}_{\boldsymbol{hh}} \triangleq \operatorname{toeplitz}\{\psi_{hh}[0], \psi_{hh}[1], \dots, \psi_{hh}[N-1]\}, \tag{5}$$

$$\tilde{\bar{\boldsymbol{S}}}_\mathrm{D}[k] \triangleq \operatorname{diag}\{\tilde{\boldsymbol{S}}[k-N+1], \dots, \tilde{\boldsymbol{S}}[k]\}, \tag{6}$$

[1]We note that (i) this assumption is made *only to simplify the receiver design* for general unitary DSTM codes and (ii) it is not an approximation for the important class of group (cyclic and dicyclic) DSTM codes [2], [3], where each antenna is active only once during N_T intervals.

with

$$\tilde{\boldsymbol{S}}[k-\kappa] \triangleq \prod_{\nu=\kappa}^{N-2} \tilde{\boldsymbol{V}}[k-\nu], \quad 0 \le \kappa \le N-2, \tag{7}$$

and $\tilde{\boldsymbol{S}}[k-N+1] = \boldsymbol{I}_{N_\mathrm{T}}$.

III. DECISION–FEEDBACK SUBSET MULTIPLE–SYMBOL DIFFERENTIAL DETECTION (DF–S–MSDD)

In this section, we present DF–S–MSDD and its TS–based implementation for low–complexity and reliable noncoherent detection.

A. Formulation of DF–S–MSDD

In [15] it was observed that symbol estimates at the edges of the MSDD observation window are less reliable than estimates for the center symbols. A modification of MSDD, so–called subset MSDD (S–MSDD) was devised, which discards those unreliable decisions. The DF–S–MSDD scheme proposed in this letter combines the general idea of S–MSDD with the concept of decision feedback from DFDD as explained in the following.

As in conventional MSDD, an observation window extending over N received symbols summarized in $\bar{\boldsymbol{R}}[k]$ is applied. Instead of optimizing the ML–MSDD metric (3) over all $N-1$ corresponding data symbols $\tilde{\boldsymbol{V}}[k-\kappa]$, $0 \le \kappa \le N-2$, $(N-\kappa_\mathrm{U}-2)$ previous decisions $\hat{\boldsymbol{V}}[k-\kappa]$, $\kappa_\mathrm{U}+1 \le \kappa \le N-2$, are fed back and the ML–MSDD metric is optimized only over the remaining $\kappa_\mathrm{U}+1$ symbols $\tilde{\boldsymbol{V}}[k-\kappa]$, $0 \le \kappa \le \kappa_\mathrm{U}$. In order to exclude the often unreliable symbols at the end of the observation window, the decoder does not return all $\kappa_\mathrm{U}+1$ decisions $\hat{\boldsymbol{V}}[k-\kappa]$, $0 \le \kappa \le \kappa_\mathrm{U}$, but only $\kappa_\mathrm{U}-\kappa_\mathrm{L}+1$ decisions $\hat{\boldsymbol{V}}[k-\kappa]$, $\kappa_\mathrm{L} \le \kappa \le \kappa_\mathrm{U}$, and discards the remaining κ_L decisions at the end of the observation window. Accordingly, the observation window must slide forward in steps of $\kappa_\mathrm{U} - \kappa_\mathrm{L} + 1$ symbols at a time. Figure 1 illustrates the use of received samples, decision feedback, and subset detection in DF–S–MSDD. The two newly introduced parameters κ_U and κ_L need to be adjusted appropriately, which will be illustrated in Section IV.

B. Tree–Search Based Implementation for DF–S–MSDD

While the use of decision–feedback symbols already lowers computational complexity of DF–S–MSDD compared to that of MSDD, further complexity reduction is desirable especially for larger values of κ_U and signal constellation sizes L. For this purpose, we devise the application of fast tree–search (TS) decoding to DF–S–MSDD.

Applying the Cholesky factorization of the inverse correlation matrix $\boldsymbol{C}^{-1} = \boldsymbol{L}^\mathsf{H}\boldsymbol{L}$ with lower triangular matrix $\boldsymbol{L}$ [19, Ch. 3.7] with elements $l_{i,j}$ in the $(i+1)$st row $(j+1)$st column, the ML–MSDD metric (3) can be rewritten as

$$\hat{\bar{\boldsymbol{V}}}[k] = \operatorname*{argmin}_{\tilde{\bar{\boldsymbol{V}}}[k]\in\mathcal{V}^{N-1}} \left\{ \sum_{\kappa=0}^{N-2} \left\| \sum_{i=\kappa}^{N-1} l_{\kappa,i}\tilde{\boldsymbol{S}}^\mathsf{H}[k-i]\boldsymbol{R}[k-i] \right\|^2 \right\}. \tag{8}$$
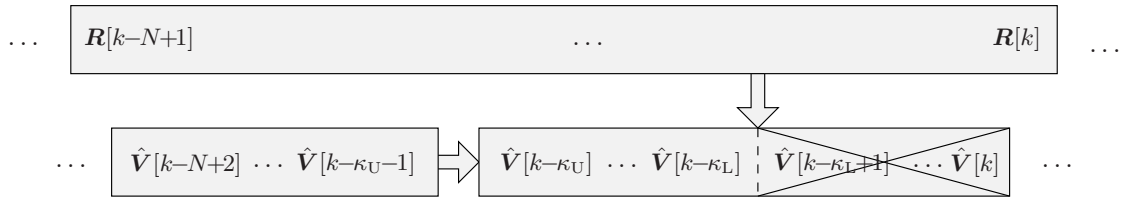
Fig. 1. Illustration of decision–feedback subset multiple–symbol differential detection (DF–S–MSDD). The observation window slides forward in steps of $\kappa_\mathrm{U} - \kappa_\mathrm{L} + 1$.

This metric expression allows application of TS decoding to perform DF–S–MSDD. In case of conventional MSDD considered in [13]–[15], the symbol $\tilde{S}[k-N+1] = I_{N_\mathrm{T}}$ corresponds to the root and the sequences $[\tilde{S}[k-N+1], \ldots, \tilde{S}[k]]$ to the leaves of a depth–$(N-1)$ decoding tree. For DF–S–MSDD, the feedback of $N - \kappa_\mathrm{U} - 2$ previous decisions $\hat{V}[k-\kappa]$, $\kappa_\mathrm{U} + 1 \leq \kappa \leq N - 2$, corresponds to fixing a node at depth $N - \kappa_\mathrm{U} - 2$ of the tree by fixing

$$\tilde{S}[k-\kappa] = \prod_{\nu=\kappa}^{N-2} \hat{V}[k-\nu], \quad \kappa_\mathrm{U} + 1 \leq \kappa \leq N - 2. \quad (9)$$

This node can be viewed as the root of a tree of depth $\kappa_\mathrm{U} + 1$, and the remaining $\kappa_\mathrm{U} + 1$ symbols $\hat{V}[k-\kappa]$, $0 \leq \kappa \leq \kappa_\mathrm{U}$, corresponding to the different levels of the tree, are found by means of TS decoding in this smaller tree. In (8) this reflects in the fact that the addends of the outer sum over κ are independent of the candidates $\tilde{V}[k-\kappa]$, $0 \leq \kappa \leq \kappa_\mathrm{U}$, and therefore irrelevant for the metric minimization in (8). Taking this into account and with the definitions

$$\breve{R}_\kappa[k-i] \quad \triangleq \quad l_{\kappa,i} R[k-i], \quad (10)$$

$$Y_\kappa \quad \triangleq \quad \sum_{i=\kappa_\mathrm{U}+1}^{N-1} \tilde{S}^\mathsf{H}[k-i] \breve{R}_\kappa[k-i], \quad (11)$$

$$X_\kappa \quad \triangleq \quad \tilde{S}[k-\kappa-1]\Big(Y_\kappa + \quad (12)$$

$$\sum_{i=\kappa+1}^{\kappa_\mathrm{U}} \tilde{S}^\mathsf{H}[k-i] \breve{R}_\kappa[k-i]\Big), \quad (13)$$

$0 \leq \kappa \leq \kappa_\mathrm{U}$, we can write the DF–S–MSDD decision rule as

$$\left[\hat{V}[k-\kappa_\mathrm{U}], \ldots, \hat{V}[k]\right] = \underset{\substack{\tilde{V}[k-\kappa] \in \mathcal{V} \\ \forall \kappa \in \{0, \ldots, \kappa_\mathrm{U}\}}}{\mathrm{argmin}} \left\{\sum_{\kappa=0}^{\kappa_\mathrm{U}} \delta_\kappa\right\} \quad (14)$$

with

$$\delta_\kappa \triangleq \left\| \tilde{V}^\mathsf{H}[k-\kappa] \breve{R}_\kappa[k-\kappa] + X_\kappa \right\|^2. \quad (15)$$

We note that all terms δ_κ in the sum in (14) are non–negative and that δ_κ only depends on $[\tilde{V}[k-\kappa], \ldots, \tilde{V}[k-\kappa_\mathrm{U}]]$. Therefore, DF–S–MSDD can be interpreted as a $(\kappa_\mathrm{U} + 1)$–dimensional tree–search problem with branch metric δ_κ. In consequence, the methods recently devised in [13]–[15] to solve the regular MSDD problem by means of TS decoding can be readily applied to efficiently solve the DF–S–MSDD problem in (14). In particular, the use of a Fano–type metric defined in the same way as for regular tree–search based MSDD in [15, Section III-B.2] is possible and will turn out

beneficial in terms of performance vs. complexity tradeoff (see the results in Section IV). Furthermore, we note that the matrices Y_κ, $0 \leq \kappa \leq \kappa_\mathrm{U}$, defined in (11) are independent of the particular candidate under consideration, which means that they need to be computed only once at the beginning of the tree search.

C. Discussion

A similar feedback–aided MSDD algorithm for DSTM has been proposed as MSD4 in [14]. There, DSTM was limited to only *diagonal* constellations, while DF–S–MSDD proposed here comprises general unitary DSTM constellations. The authors suggested to feed back $N - 2 - \kappa_\mathrm{U}$ previously detected symbols and return decisions on *all* remaining $\kappa_\mathrm{U} + 1$ data symbols in the observation window. Therefore, MSD4 can be considered as a special case of DF–S–MSDD with $\kappa_\mathrm{L} = 0$, and as such it is strictly inferior to conventional MSDD applying the same window size N. DF–S–MSDD, on the other hand, typically achieves an error–rate performance close to that of S–MSDD, which is better than that of MSDD. This is true especially in rapid fading scenarios, where the error rate of conventional MSDD is degraded severely by unreliable decisions at the edges of the observation window. At the same time, computational complexity is significantly reduced compared to MSDD and S–MSDD as the dimension of the search space is $\kappa_\mathrm{U} + 1$ instead of $N - 1$, i.e. there are $L^{\kappa_\mathrm{U}+1}$ relevant candidates instead of L^{N-1}.

Furthermore, it is clear from the problem formulation of MSDD that DF–S–MSDD is related to well–known sequential and reduced–state algorithms used for sequence estimation for coded transmission and transmission over intersymbol–interference channels, cf. e.g. [20], [21]. We note that this is true for (almost) all improved noncoherent receivers, and the actual task in noncoherent detection is to devise schemes with favorable tradeoffs between detection complexity and error–rate performance. As we exemplarily show in the next section, the proposed DF–S–MSDD achieves the best performance–complexity tradeoff among the improved detectors for DSTM.

Finally, we note that for a quick *approximation* of the symbol–error rate of DF–S–MSDD the expression

$$\mathrm{SER} \approx \frac{1}{\kappa_\mathrm{U} - \kappa_\mathrm{L} + 1} \sum_{\kappa=\kappa_\mathrm{L}}^{\kappa_\mathrm{U}} \mathrm{SER}_{N-1-\kappa}, \quad (16)$$

could be evaluated, where SER_n are the SERs in the individual positions of the MSDD observation window according to [15, Eq. (26)]. In doing so, error-free feedback needs to be
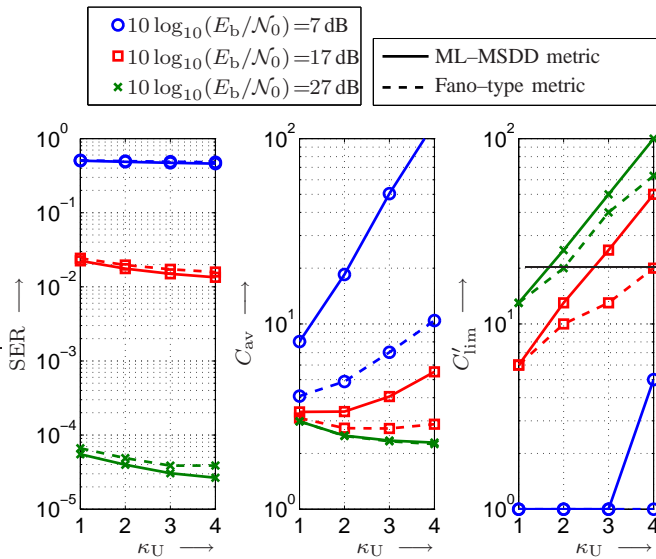
Fig. 2.   Results for DF–S–MSDD with $\kappa_{\mathrm{L}} = 1$ and different values of κ_{U}. Left: SER, center: average complexity C_{av}, right: minimal allowed limiting complexity C'_{lim} (see text). With ML–MSDD metric (solid lines) and with Fano–type metric (dashed lines).

Fig. 3.   Comparison of various detectors with respect to SER vs. $E_{\mathrm{b}}/\mathcal{N}_0$.

assumed, which results in some underestimation of the true error rate. We therefore present simulation results to discuss the actual performance of DF-S-MSDD in the next section.

IV. NUMERICAL RESULTS AND DISCUSSION

In this section, we show simulation results to illustrate the error–rate performance and the complexity of DF–S–MSDD. For this purpose, we consider a system with the following parameters as an example: $N_{\mathrm{T}} = 3$ transmitter and $N_{\mathrm{R}} = 1$ receiver antennas, diagonal DSTM with $R = 2$ (and therefore $L = 64$) according to [3, Table I], Clarke's fading with normalized fading bandwidth $B_h T = 0.03$, i.e. $\psi_{hh}[\kappa] = \mathrm{J}_0(0.06\pi N_{\mathrm{T}}\kappa)$, where $\mathrm{J}_0(x)$ denotes the 0th–order Bessel function of the 1st kind, and an observation window length $N = 10$. As benchmark detectors, we consider conventional differential detection (CDD, $N = 2$), DFDD, conventional MSDD, S–MSDD, MSD4, and (differentially) coherent detection with perfect channel state information (CSI). All schemes are implemented with the efficient TS decoding from [15, Section III-B] and with lattice–detector (LD) based symbol search, cf. [15], [22], [23]. In case of MSD4, this TS decoding is preferable in terms of performance–complexity tradeoff to the bound–intersection detection (BID) based algorithms originally suggested for MSD4 in [14]. Furthermore, besides the ML–MSDD metric, TS decoding with the Fano–type metric (cf. [15, Section III-B.2]) is also used. As a simple measure of computational complexity, we consider the number of examined nodes in the tree per decoded symbol.

Let us first discuss appropriate choices for the parameters κ_{U} and κ_{L}. We overall found that using $\kappa_{\mathrm{L}} = 1$, i.e. only the decision for the last symbol in the observation window is discarded, yields almost all the achievable gain in error–rate performance over conventional MSDD while minimizing
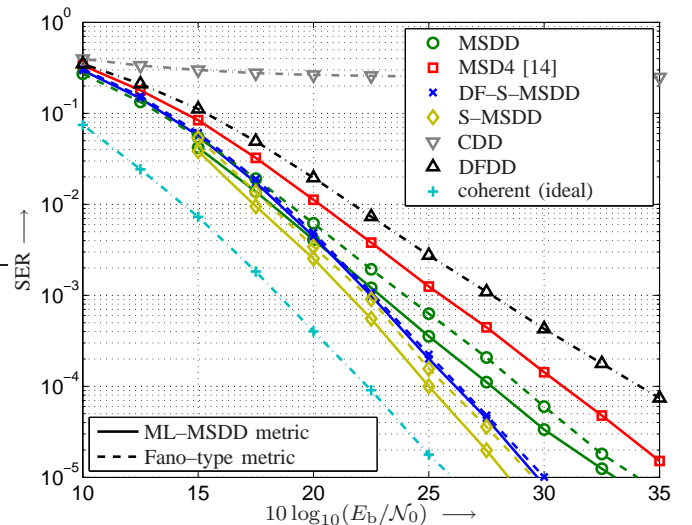
the overlap between consecutive observation windows. This coincides with the findings in [24], where it was shown that in fast–fading scenarios the reliability of the decisions is roughly independent of the position in the observation window with the exception of the edge positions. Fixing $\kappa_{\mathrm{L}} = 1$, Figure 2 shows (i) the symbol–error rate (SER) (left), (ii) the average number C_{av} of examined nodes per decoded symbol (center), and (iii) a quantity C'_{lim} defined as the minimal number of examined nodes per decoded symbol, after which the tree search can be terminated without noteworthy impact on the SER.[2] Solid lines indicate the use of the ML– MSDD metric, whereas dashed lines correspond to the Fano– type metric. Three different SNR values are considered (E_{b} and $\mathcal{N}_0$ denote the received energy per information bit and the two–sided noise–power spectral density in the equivalent complex baseband, respectively). The SER results in the left subplot show that the performance somewhat improves if κ_{U} is increased, which is due to a slightly improved reliability of the decisions towards the center of the observation window and reduced error propagation if fewer previous decisions are fed back into the DF–S–MSDD metric. The results for C_{av} show that for relatively low SNR the average complexity of DF– S–MSDSD exhibits the behavior typical for TS algorithms, i.e. the complexity is an increasing function of the tree depth $\kappa_{\mathrm{U}}+1$. In high SNR, on the other hand, the average complexity of DF–S–MSDD even decreases with growing κ_{U}, as here the average complexity per decoded symbol of (unlimited) DF–S–MSDD is close to its minimum of $2 + 1/\kappa_{\mathrm{U}}$. Finally, the results for C'_{lim} clearly show that small values of κ_{U} are preferable. With $\kappa_{\mathrm{U}} = 1$ we can see that the tree search can be terminated after only 6 (at 17 dB) to 13 (at 27 dB) examined candidates per decoded symbol without noteworthy impact on the error–rate performance, while a full search would examine $L^2 = 4096$ candidates to achieve the same performance. (We note that, since the SER at $E_{\mathrm{b}}/\mathcal{N}_0 = 7$ dB is about 0.5, the

---

[2]More specifically, C'_{lim} is determined such that the SER is increased by no more than a factor of 1.1 compared to the unlimited search.
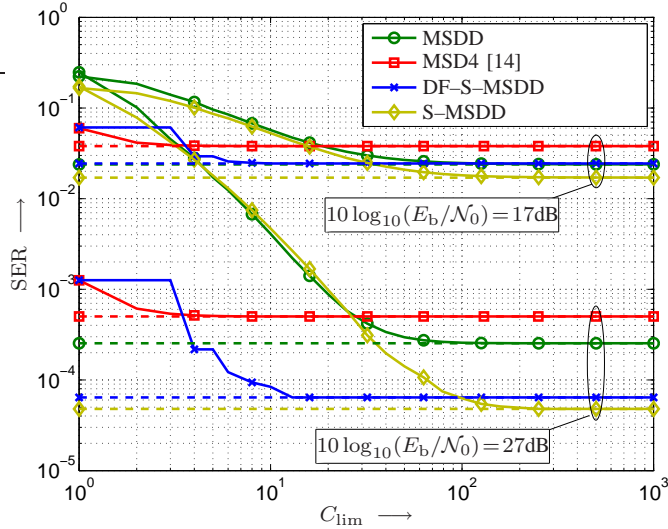
Fig. 4. Performance vs. maximal allowed complexity C_{lim} per decoded symbol for different SNRs $10\log_{10}(E_{\text{b}}/\mathcal{N}_0)$. Dashed lines: SER when $C_{\text{lim}} \to \infty$. TS decoding with Fano–type metric is applied.

complexity curves for this case are only included to illustrate the trend with increasing SNR.)

In summary, it can be concluded that $\kappa_{\text{U}} = \kappa_{\text{L}} = 1$, i.e. the tree searched in DF–S–MSDD is of depth two, leads to a very favorable performance–complexity tradeoff regardless of the SNR. Hence the following comparisons with benchmark detectors we consider $\kappa_{\text{U}} = \kappa_{\text{L}} = 1$.

Figure 3 compares the error–rate performance of the various detectors. Both ML and Fano–type metric are considered. MSD4 uses $N-3$ feedback symbols (like DF–S–MSDD) and returns decisions for the last two symbols in the observation window. We observe that MSDD clearly outperforms DFDD and CDD, which suffers from a very high error floor. It can further be seen that the use of the Fano–type metric results in relatively small performance losses of about $0.5-1.0\,\text{dB}$. Interestingly, the performance loss due to the Fano–type metric is almost negligible for DF–S–MSDD, which can be attributed to the very low dimension (two) of the TS decoding problem in this case. This way, DF–S–MSDD with Fano–type metric achieves almost the same performance as S–MSDD, which is within approximately 3 dB of idealized coherent detection, while MSD4 (with ML and Fano–type metric) operates at a significantly higher SNR compared to S–MSDD due to the poor reliability of the last decision in the observation window.

In Figure 4 we consider the performance that can be achieved if the maximal number of examined candidates per decoded symbol is limited to a finite C_{lim}, i.e. if the TS process is terminated after $(N-1)C_{\text{lim}}$ (MSDD), $(\kappa_{\text{U}} - \kappa_{\text{L}} + 1)C_{\text{lim}}$ (DF–S–MSDD), $2C_{\text{lim}}$ (MSD4) and $(N-3)C_{\text{lim}}$ (S–MSDD) examined candidates. The Fano–type metric is applied for all detectors. The dashed horizontal lines mark the SER when $C_{\text{lim}} \to \infty$. We observe that the maximal instantaneous complexities necessary to avoid performance degradations compared to $C_{\text{lim}} \to \infty$ are much larger for MSDD and S–MSDD than for the new DF–S–MSDD. For example, $C_{\text{lim}} = 4$ and $C_{\text{lim}} = 10$ are sufficient for DF–S–MSDD at $E_{\text{b}}/\mathcal{N}_0 =$
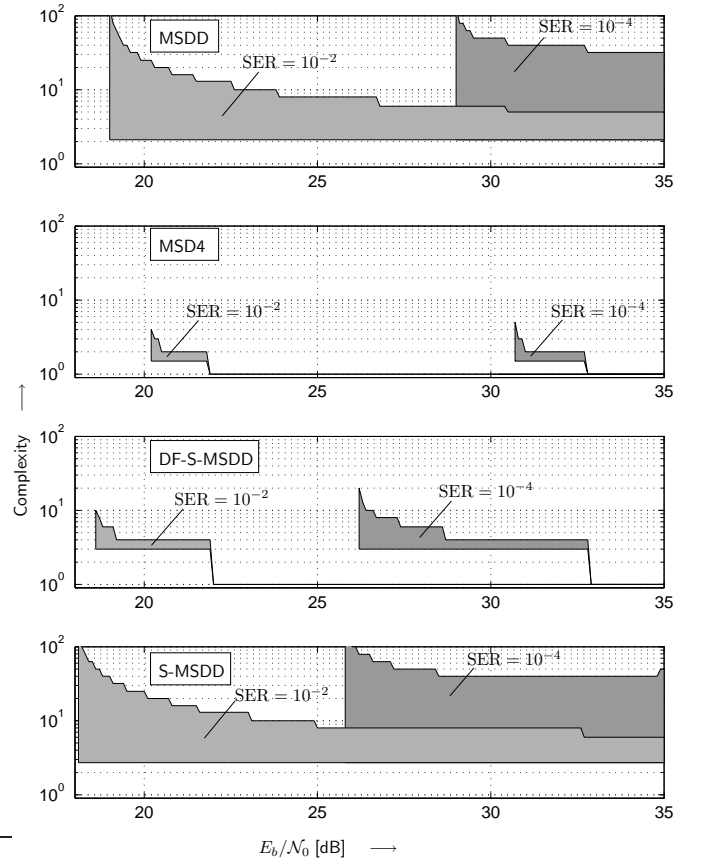
Fig. 5. Complexity range (number of examined candidates per decoded symbol) required to achieve an SER of 10^{-2} and 10^{-4}, respectively, vs. SNR $10\log_{10}(E_{\text{b}}/\mathcal{N}_0)$ for different detectors. TS decoding with Fano–type metric is applied.

17 dB and 27 dB, respectively, while $C_{\text{lim}} = 80\ldots100$ has to be allowed for MSDD and S–MSDD. Although the maximal required complexity of MSD4 is slightly below that of S–DF–MSDD, the performance saturates at considerably higher error rates (as also shown in Figure 3).

Finally, Figure 5 compares the complexities required to achieve an SER of, respectively, 10^{-2} and 10^{-4} as function of the SNR. Since the instantaneous complexity is a random variable depending on the channel and noise realization, Figure 5 shows the measured ranges of complexity. The left boundaries of the shaded areas indicate the cutoff SNRs below which the target SERs cannot be achieved. It can be seen that the cutoff SNRs for DF–S–MSDD are much lower than those for MSDD and MSD4, and very close to those for S–MSDD. At the same time the complexities for DF–S–MSDD extend over significantly smaller ranges with much lower absolute values than those for S–MSDD and MSDD, and are quite comparable to those for MSD4. Thus, this figure nicely illustrates that DF–S–MSDD offers the best performance–complexity tradeoff among the different detectors.

V. CONCLUSIONS

In this letter, we have introduced a novel noncoherent detection algorithm for DSTM, which we have named DF–S–MSDD. It combines ideas of DFDD and subset MSDD by

feeding back a number of previous decisions into the MSDD metric, optimizing the latter only over the remaining symbols, and returning decisions only on a subset of these symbols. Due to the relationship with subset MSDD error–rate performances even better than those of MSDD are feasible, especially in rapid fading environments. At the same time, the reduction of the search space dimension in conjunction with an appropriate implementation based on tree–search decoding results in a very low average complexity, and instantaneous complexity can be limited to very small values without affecting detector performance. This is true for a relatively wide range of relevant SNRs and constitutes an important advantage over existing TS–based MSDD algorithms.

REFERENCES

[1] V. Tarokh and H. Jafarkhani. A Differential Detection Scheme for Transmit Diversity. *IEEE J. Select. Areas Commun.*, 18(7):1168–1174, July 2000.

[2] B. L. Hughes. Differential Space–Time Modulation. *IEEE Trans. Inform. Theory*, 46(7):2567–2578, November 2000.

[3] B. M. Hochwald and W. Sweldens. Differential Unitary Space–Time Modulation. *IEEE Trans. Commun.*, 48(12):2041–2052, December 2000.

[4] S. T. Andersson and N. A. B. Svensson. Noncoherent Detection of Convolutionally Encoded Continuous Phase Modulation. *IEEE J. Select. Areas Commun.*, 7(9):1402–1414, December 1989.

[5] J. H. Lodge and M. L. Moher. Maximum Likelihood Sequence Estimation of CPM Signals Transmitted Over Rayleigh Flat–Fading Channel. *IEEE Trans. Commun.*, 38:787–794, June 1990.

[6] G. M. Vitetta and D. P. Taylor. Viterbi Decoding of Differentially Encoded PSK Signals Transmitted over Rayleigh Frequency–Flat Fading Channels. *IEEE Trans. Commun.*, 43(2/3/4):1256–1259, February/March/April 1995.

[7] G. Colavolpe and R. Raheli. Noncoherent Sequence Detection. *IEEE Trans. Commun.*, 47(9):1376–1385, September 1999.

[8] E. Chiavaccini and G. M. Vitetta. Further Results on Tarokh's Space–Time Differential Technique. In *Proc. of IEEE International Conference on Communications (ICC)*, New York, April-May 2002.

[9] C. Ling, K. H. Li, and A. C. Kot. Noncoherent Sequence Detection of Differential Space–Time Modulation. *IEEE Trans. Inform. Theory*, 49(10):2727–2734, October 2003.

[10] S. G. Wilson, J. Freebersyser, and C. Marshall. Multi–Symbol Detection of M–DPSK. In *Proc. of IEEE Global Telecommunications Conference (Globecom)*, pages 47.3.1–47.3.6, Dallas, November 1989.

[11] D. Makrakis and P. T. Mathiopoulos. Optimal Decoding in Fading Channels: A Combined Envelope, Multiple Differential and Coherent Detection Approach. In *Proc. of IEEE Global Telecommunications Conference (Globecom)*, pages 1551–1557, Dallas, November 1989.

[12] D. Divsalar and M. K. Simon. Multiple–Symbol Differential Detection of MPSK. *IEEE Trans. Commun.*, 38(3):300–308, March 1990.

[13] P. Pun and P. Ho. Fano Space–Time Multiple Symbol Differential Detectors. In *Proc. of IEEE Global Telecommunications Conference (Globecom)*, pages 3169–3174, Saint Louis, November 2005.

[14] T. Cui and C. Tellambura. Bound–Intersection Detection for Multiple–Symbol Differential Unitary Space–Time Modulation. *IEEE Trans. Commun.*, 53(12):2114–2123, December 2005.

[15] V. Pauli and L. Lampe. Tree–Search Multiple–Symbol Differential Decoding for Unitary Space–Time Modulation. *IEEE Trans. Commun.*, 55(8):1567–1576, August 2007.

[16] H. Leib and S. Pasupathy. Optimal Noncoherent Block Demodulation of Differential Phase Shift Keying (DPSK). *Archiv für Elektronik und Übertragungstechnik*, 45(5):299–305, 1991.

[17] A. Svensson. Coherent Detection Based on Linear Prediction and Decision Feedback for QDPSK. *IEE Electronics Letters*, 30(20):1642–1643, 1994.

[18] C. Ling, K. H. Li, and A. C. Kot. On Decision–Feedback Detection of Differential Space–Time Modulation in Continuous Fading. *IEEE Trans. Commun.*, 52(10):1613–1617, October 2004.

[19] S. Haykin. *Adaptive Filter Theory*. Prentice–Hall, Englewood Cliffs, NJ, third edition, 1996.

[20] J. B. Anderson and S. Mohan. Sequential Coding Algorithms: A Survey and Cost Analysis. *IEEE Trans. Commun.*, 32(2):169–176, February 1984.

[21] M. V. Eyuboğlu and S. U. H. Qureshi. Reduced–State Sequence Estimation with Set Partitioning and Decision Feedback. *IEEE Trans. Commun.*, 36(1):13–20, January 1988.

[22] K. L. Clarkson, W. Sweldens, and A. Zheng. Fast Multiple Antenna Differential Decoding. *IEEE Trans. Commun.*, 49(2):253–261, February 2001.

[23] C. Ling, W. H. Mow, K. H. Li, and A. C. Kot. Multiple–Antenna Differential Lattice Decoding. *IEEE J. Select. Areas Commun.*, 23:1821–1829, September 2005.

[24] V. Pauli, R. Schober, and L. Lampe. A Unified Performance Analysis Framework for Differential Detection in MIMO Rayleigh Fading Channels. *IEEE Trans. Commun.*, To be published 2008.